

Association between cloud radiative forcing and general circulation in East Asia summer monsoon

Wei-Chyung Wang, Chao-Tzuen Cheng(1)

Atmospheric Sciences Research Center, State University of New York, Albany

QingYun Zhang(2)

Institute of Atmospheric Physics, Chinese Academy of Sciences, Beijing

Huang-Hsiung Hsu(3), Chihua Wu(3) and Wen-Shung Kau(3)

Department of Atmospheric Sciences, National Taiwan University, Taipei

1. Introduction

The East Asia summer monsoon (EASM) exhibits distinctive characteristics of large cloud amounts with associated heavy and persistent rainfall, although occasional breaks occur. Therefore, cloud-radiation interaction is an important aspect of the cloud-climate interaction. Wang et al. (2003) used the cloud radiative forcing (CRF) as a diagnostic parameter for conducting model-observation comparison. CRF at the top of the atmosphere, a “macroscopic parameter” incorporating all aspects of the radiative effect of cloud (the cover, liquid/ice water, microphysical properties, cloud vertical overlapping), includes two components: the shortwave (SW) and longwave (LW) CRF.

In Wang et al. (2003), we used both observed and AMIP-II model simulated East Asian summer monsoon to study the spatial and temporal patterns of SW- and LW-CR, and the association between CRFs and cloud properties (cloud cover and cloud water). The observational analyses, shown in Fig. 1, indicate that the CRF is dominated by the SW-CRF, in particular for the Yangtze-Huai River valley (YHRV) during May and June, while the LW-CRF shows a weak dependence on the latitudes and seasons. Different seasonal characteristics are present for Northern China in both SW- and LW-CRF variations. However, the most interesting feature, from a large-scale perspective, is that the SW-CRF over YHRV is significantly stronger than the respective Northern Hemisphere zonal mean value, thus implying a very different vertical distribution of cloud properties between the two regions. Wang et al. (2003) also find that there exists a close association between LW-CRF and high cloud cover, and between

SW-CRF and total cloud cover. On the other hand, simulations from ECHAM and SUNYA-CCM3, also shown in Fig. 1, indicate qualitative agreement with observations, although the magnitude is different and the difference is a strong function of seasons and latitudes. In addition, as illustrated in Fig. 1, over YHRV [and same as in South China (not shown)], the 1985-89 ERBE data shows a significant, $\sim 45 \text{ Wm}^{-2}$, decrease in NET-CRF from May to August. The decrease is dominated, $\sim 80\%$, by decreases in SW-CRF.

The present study is an extension of Wang et al. (2003) with focus on the association in the spatial and temporal characteristics of CRF with large-scale circulation and moisture transport. Specifically, we study the association in May and August, the two months in which a significant decrease in CRF cooling occurs in both the South China and YHRV.

2. Diagnostic Study

Results are presented here to illustrate the consistency and associations between the CRFs and general circulation, with “notes” added to highlight the study findings.

3. Conclusions and Discussion

The significant decreases in the cloud radiative forcing over Yangtze-Huai River valley between May and August are consistent with changes in cloud radiative properties observed from ISCCP, showing a decrease in both the total cloud cover (mainly attributed to decreases in both high and middle level cloud cover), and the cloud opacity.

Notable circulation changes between May and August include:

- Increased 850 mb specific humidity;
- Changes in 850 mb moisture transport from southwest to south with smaller intensity;
- Consistent horizontal and vertical moisture flux divergence and vertical heating/cooling distribution related to cloud vertical structure changes.

We plan to further conduct the diagnostic study on the climate model simulations relating the cloud radiative forcing to large-scale circulation. Off-line

calculations of the radiative forcing using the model simulated cloud properties and relevant climate parameters to test the sensitivity of cloud forcing to vertical cloud overlapping will also be carried out.

References

Wang, W.-C., W.-S. Kau, H.-H. Hsu, and C.-H. Tu, 2003: Characteristics of cloud radiative forcing over East Asia. *J. Climate*, EAC Special Issue (in press).

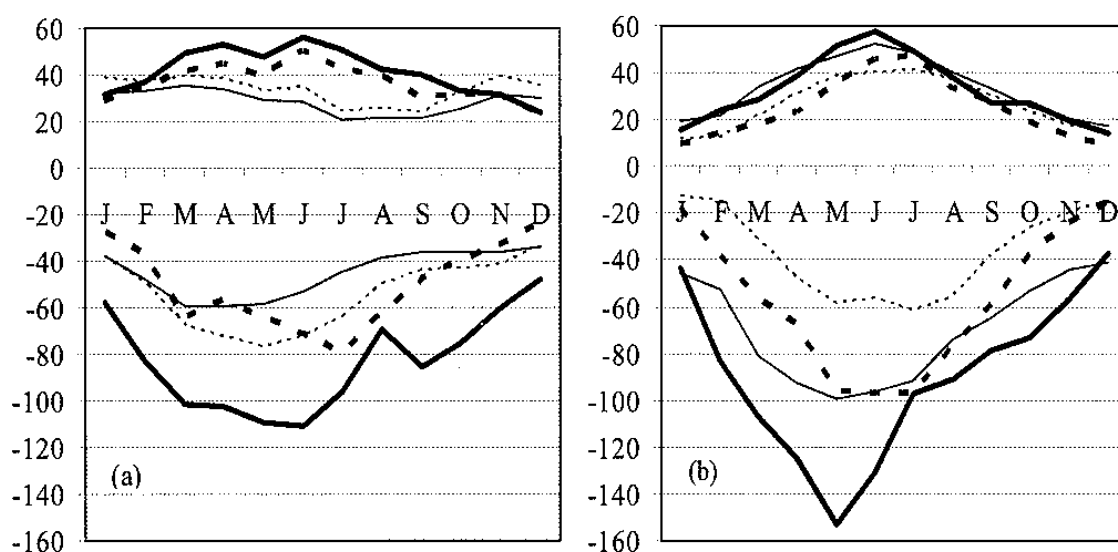


Figure 1. Annual cycle of longwave (positive) and shortwave (negative) cloud radiative forcing (Wm^{-2}) averaged over 1985-89. The lines are: thick solid for Yangtze-Huai River Valley [YHRV (105-123°E; 30-34°N)] and thick dash for North China (105-123°E; 34-43°N) (a) ERBE data: The thin solid and dashed lines correspond respectively to Northern Hemispheric zonal means of 30-34°N and 34-43°N to show their contrast to the respective YHRV and North China regions; and (b) AMIP models: The thick lines are for SUNYA-CCM3 and thin lines are for ECHAM4. [After Wang et al. (2003)]

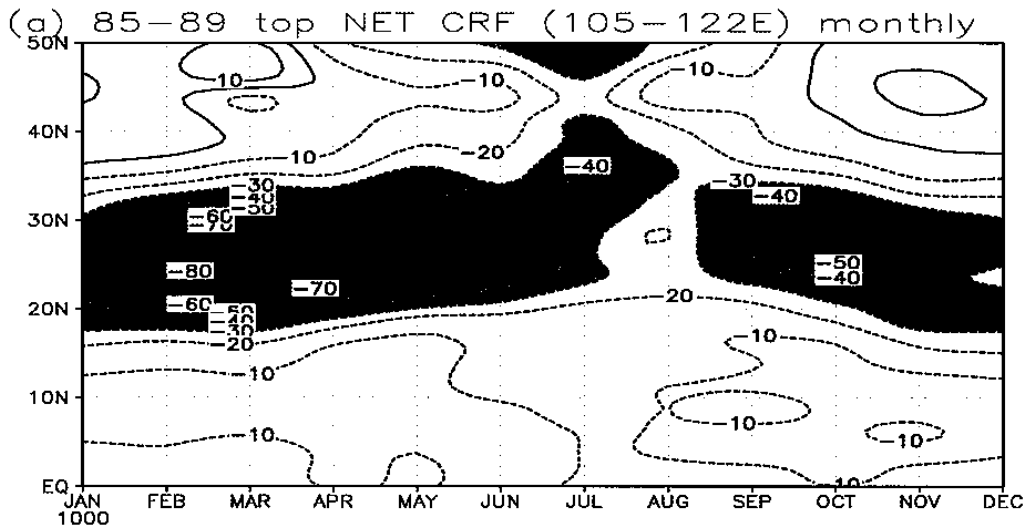


Fig. 2. Monthly and zonal (105-122°E) mean net (LW and SW) CRF (Wm^{-2}) at the top of the atmosphere from the 1985-1989 ERBE data. Note that there exist substantial cooling within 20-30 °N at spring and fall and 30-40 °N in summer.

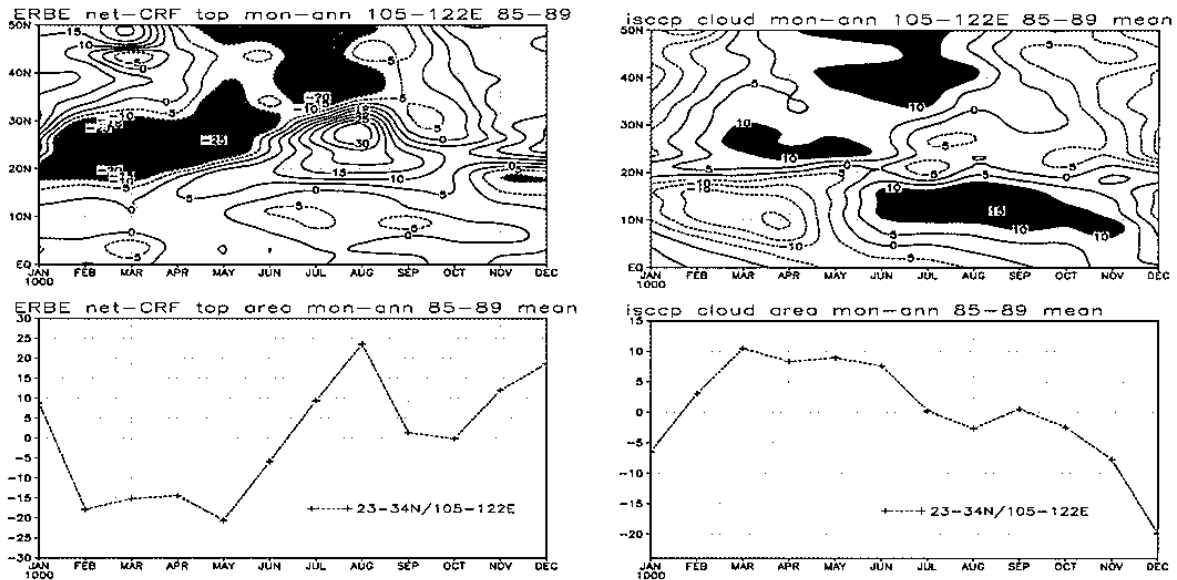


Fig. 3 *Top panels*: Monthly and zonal (105-122 °E) mean anomalies in net CRF (Wm^{-2} ; left) and total cloud cover (%; right). Note that consistent patterns in the spatial and temporal variations of CRF and total cloud cover exist, in particular over the 20-40 °N latitudes. *Bottom panels*: Monthly and regional (Yangtze-Huei River Valley; 105-122 °E, 23-34 °N) mean anomalies in net CRF (Wm^{-2} ; left) and total cloud cover (%; right). Note that the large decrease in the magnitude of the CRF from May to August is also consistent with the decrease in the total cloud cover.

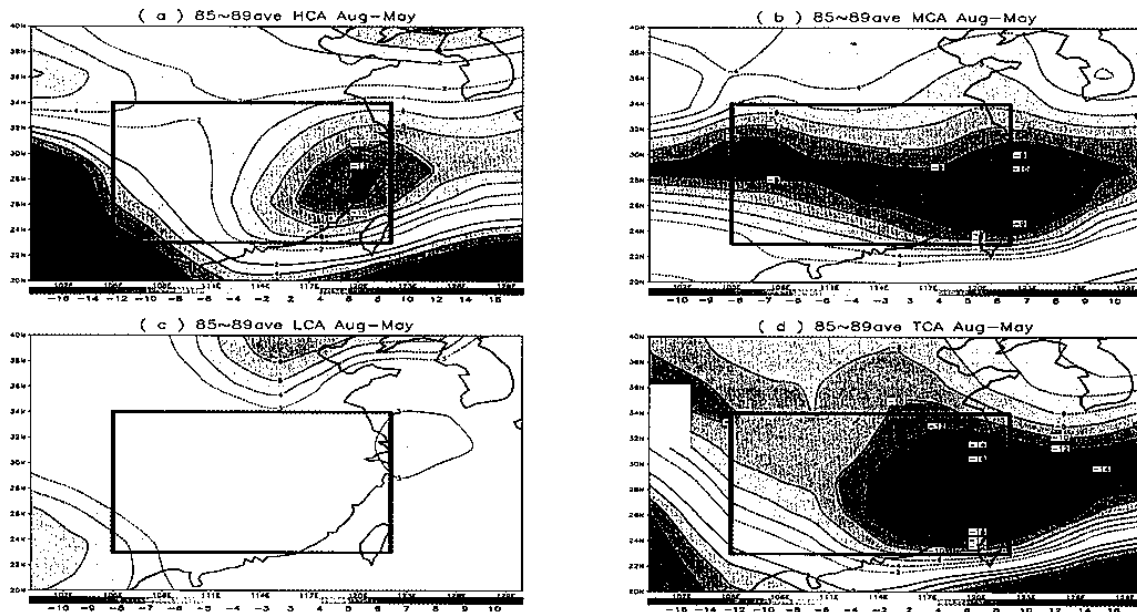


Fig.4. Difference in the 1985-89 ISCCP mean cloud cover between May and August for high, middle and low clouds, as well as the total cloud cover. Note that difference in the high and middle level clouds dominate the difference in the total cloud cover over the central marked region.

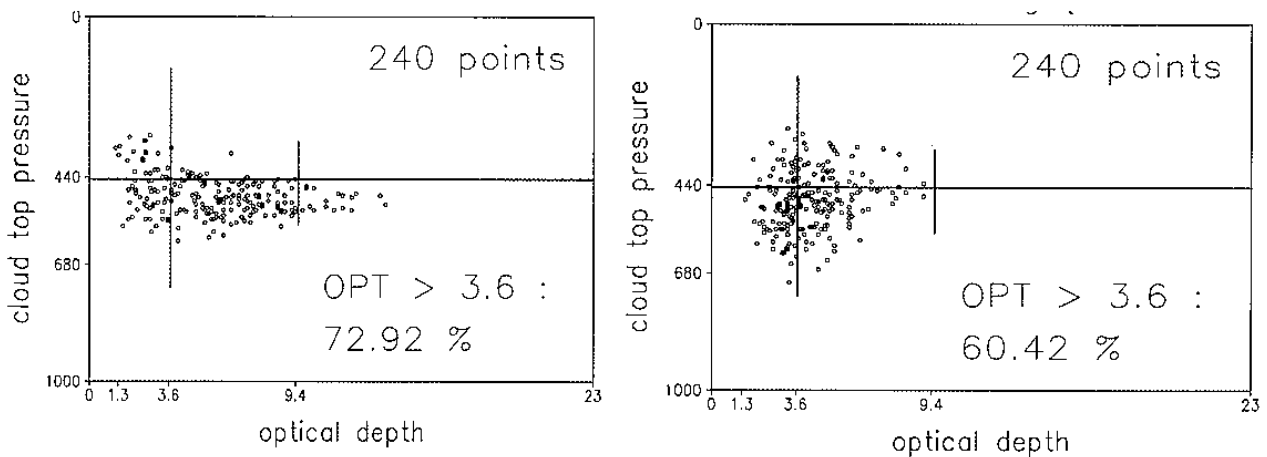


Fig. 5. The association between the cloud optical depth and cloud top pressure for the region (105~122 °E, 20~30 °N) for May (left panel) and August (right panel) derived from ISCCP data. Note that the characteristics between May and August are quite different with the tendency of higher cloud top and smaller opacity in August; for example, more high clouds exist at pressure levels <440 hPa with less opacity.

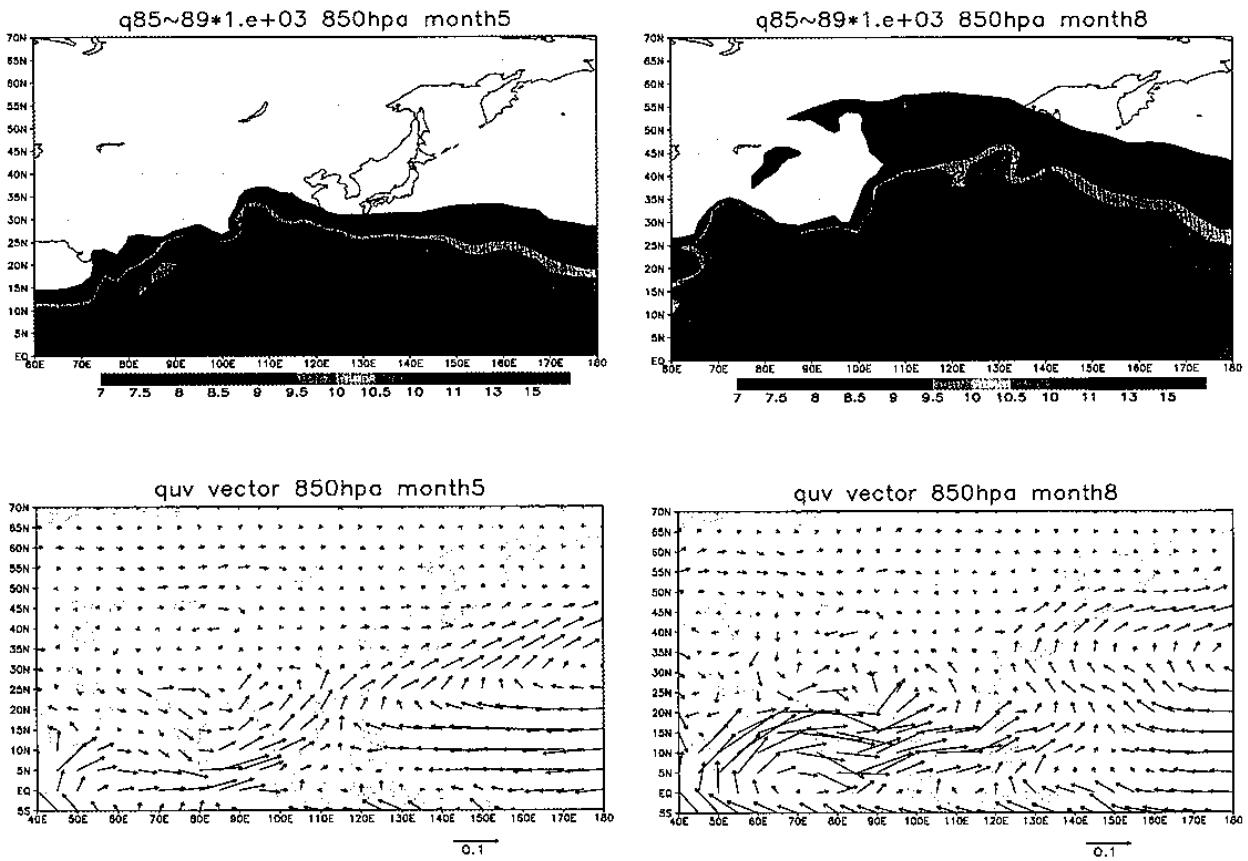


Fig. 6. Monthly mean, geographical distribution of 850 hPa specific humidity (upper panels) and moisture flux (lower panels) for May (left panel) and August (right panel). Note that there is an increase in both parameters from May to August over YHRV.

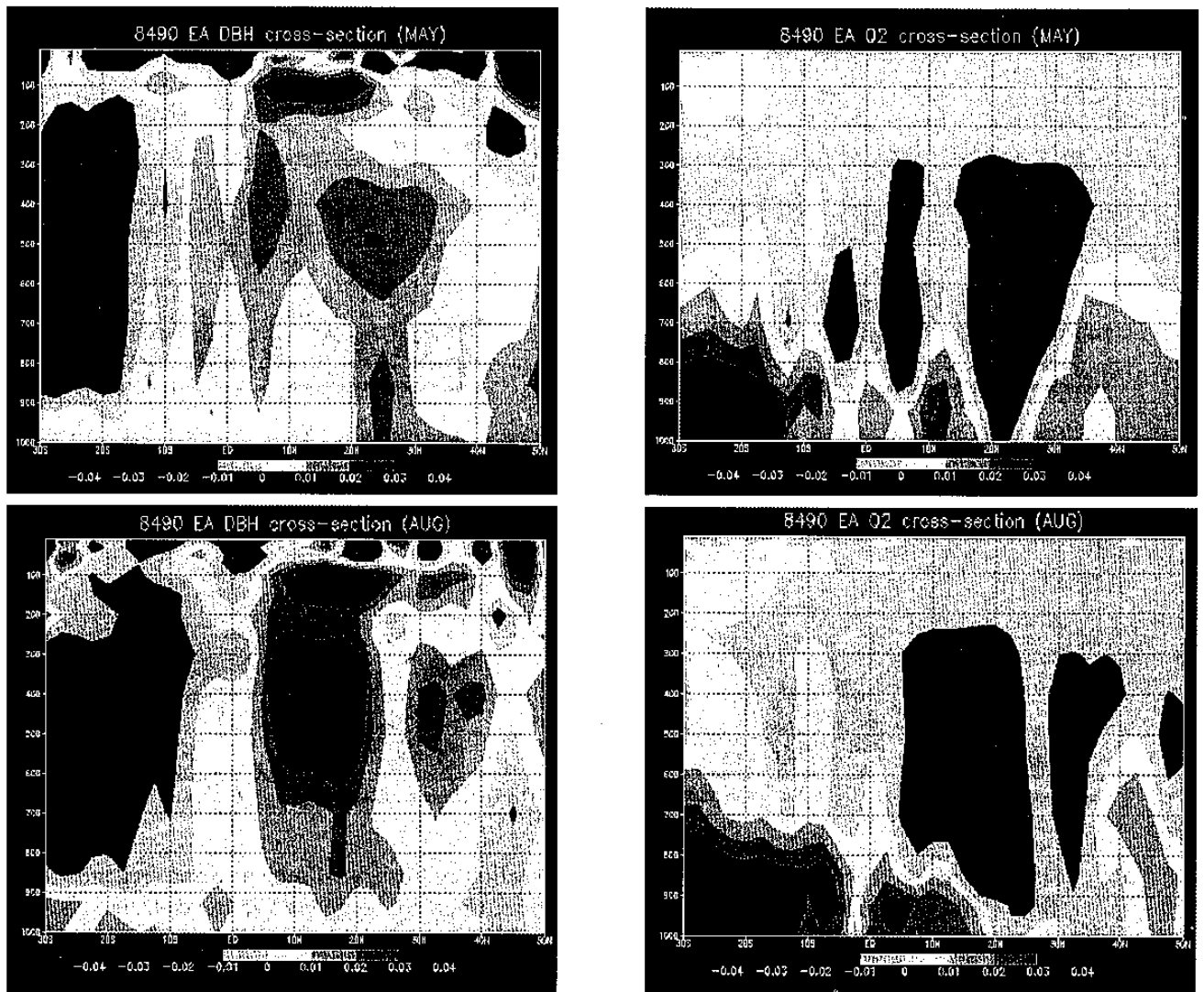
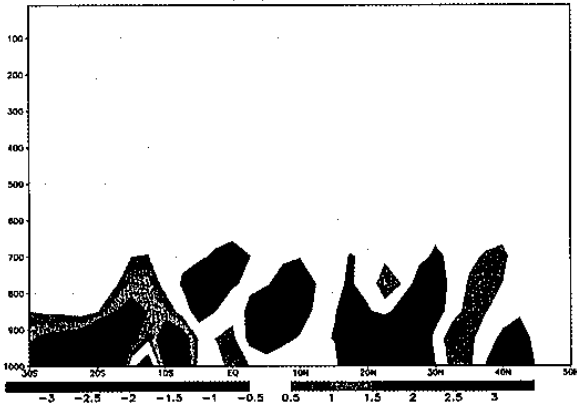
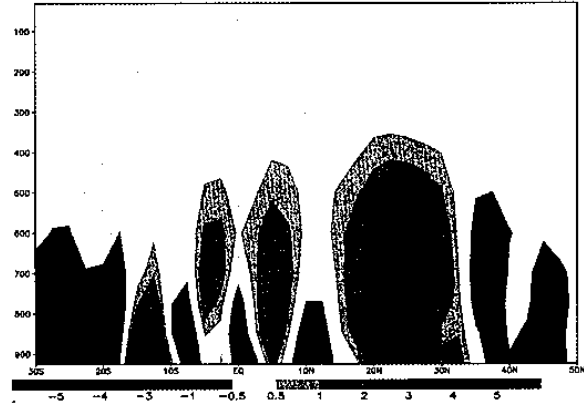


Fig.7. *Upper panels:* Latitudinal, vertical cross section of Q_1 for May (left panel) and August (right panel). Note that the near surface and mid-tropospheric heating between 20-30 °N in May are replaced by two deep convection bands over 0-20 °N and 40-50 °N in August. *Lower panels:* Same as in the upper panels except for Q_2 . Note that the moisture sink in 20-30 °N bands in May is replaced by two bands of moisture sink over 0-20 °N and 40-50 °N, which are consistent with the characteristics of Q_1 .

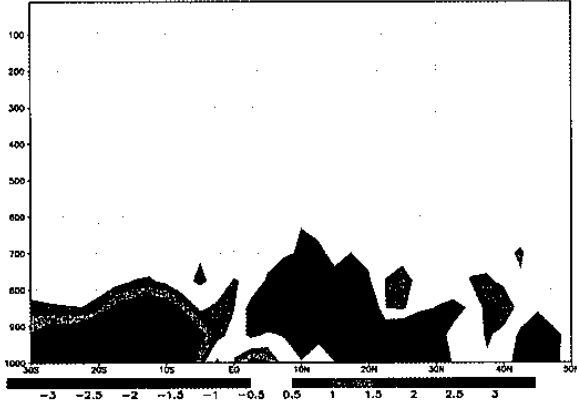
month5*1e+08 div. of qu,qv N-S vertical profile(105E~120E)



month5*1e+04 qw N-S vertical gradient 105E~120E



month8*1e+08 div. of qu,qv N-S vertical profile(105E~120E)



month8*1e+04 qw N-S vertical gradient 105E~120E

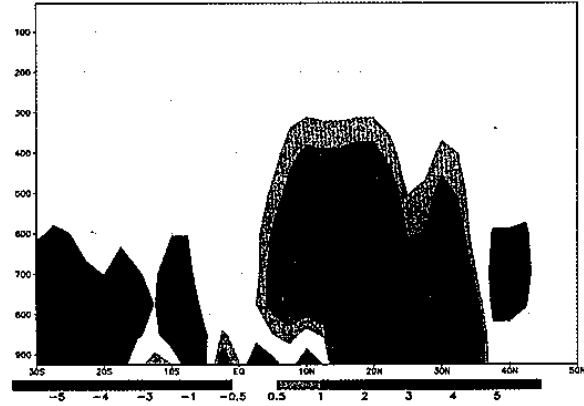


Fig.8. *Upper panels:* Latitudinal, vertical cross section of horizontal moisture convergence for May (left) and August (right). Note that the near surface convergence and lower-tropospheric divergence 20-30 °N exist in May, and the former convergence starts splitting in June (not shown) and maintains in August with the largest convergence in 10-25 °N, which is consistent with Q_1 and Q_2 .

Lower panels: Same as in the upper panels except of $d(-wq)/dp$ (w : omega), the vertical moisture transport. Note that the largest positive values appearing in 20-30 °N band in May is consistent with the moisture convergence near surface and divergence in the lower troposphere. Two bands of positive values appear in 0-20 °N and 40-50 °N bands, which are also consistent with Q_1 , Q_2 , and the horizontal convergence.